

Cite this: *J. Mater. Chem. B*, 2017,
5, 5433

Black phosphorus quantum dot based novel siRNA delivery systems in human pluripotent teratoma PA-1 cells†

Feng Yin,^{‡a} Kuan Hu,^{‡a} Si Chen,^{‡b} Dongyuan Wang,^a Jianing Zhang,^a
Mingsheng Xie,^a Dan Yang,^a Meng Qiu,^b Han Zhang,^b and Zi-gang Li^{*a}

As a novel semiconducting material, the inherent, direct, and appreciable band gap endows BP with preferable optical and electronic properties other than graphene and transition metal dichalcogenides. In addition, bio-related applications with equal importance also attract great attention thanks to several inherited advantages of BP including large drug loading capacity, high PDT efficiency, high biocompatibility and degradability. However, to date there is limited research about the biomedical applications of BP. In this study, we reported the engineering of polyelectrolyte polymers coated BP quantum dots (BP-QDs)-based nanocarriers to deliver small interfering RNA (siRNA) into human ovarian teratocarcinoma PA-1 cells. Compared to the commercial delivery reagents, superior transfection efficiency of BP-QD was detected. The expression of the LSD1 (lysine-specific demethylase 1) mRNA in PA-1 cells was significantly suppressed by BP-QDs-LSD1 siRNA complex. Notably, BP-QDs possess excellent biocompatibility and low cytotoxicity even at concentrations as high as 5 mg mL⁻¹. The combination treatment of BP nanodots-LSD1 siRNA complex with NIR light could inhibit the cell growth rate by more than 80%. In conclusion, this is the first application of BP-QDs as gene delivery systems, which shows promising potential for siRNA delivery and photothermal effects in cancer therapy.

Received 19th April 2017,
Accepted 13th June 2017

DOI: 10.1039/c7tb01068k

rsc.li/materials-b

1. Introduction

Since the first report of two-dimensional black phosphorus (BP) as a nanoelectronic device in 2014,¹ BP has been extensively studied as a promising functional material for telecommunications^{2,3} and electronics.^{4,5} As a novel semiconducting material, the inherent, direct, thickness modulated and appreciable band gap endows BP with preferable optical and electronic properties other than graphene and transition metal dichalcogenides.^{4,6} Due to its unique optical properties, higher specific surface areas and thinner sheet structures, graphene has been considered as an ideal gene delivery system in comparison with other nanomaterials in the biomedical field. However, the metabolism and toxicity of GO *in vivo* are disconcerting and thus should be explored explicitly for further clinical applications.

To date, BP has attracted much more attention in biomedical applications,^{7,8} and the main reason is that BP can be oxidized and degraded into phosphate and phosphite ions in the physiological environment, with better biocompatibility and biosafety for the human body than inorganic materials. Meanwhile, due to its unique electronic characteristics, BP can be used as a highly efficient photosensitizer for PDT applications. In addition, the absorption of BP can cover the entire visible range, enabling BP to have potent photothermal effects in cancer therapies.^{8,9}

Recently, we and co-workers reported the synergistic photodynamic/photothermal/chemotherapy of cancer based on BP nanosheets as a drug delivery system.^{10,11} These studies open up new perspectives for the design of a multifunctional nanomedicine platform based on BP nanosheets, with a high drug loading capacity and an enhanced chemotherapeutic effect. Besides the 2D layered BP structure, ultra-small BP quantum dots (BP-QDs) show a flash memory effect with a high ON/OFF current ratio, which has promising applications in electronics, solar cells, sensing and bio-imaging.^{4,7,8,12,13} Due to the wide spectral range from the visible to the near and mid-infrared region (NIR and MIR), BP-QDs have been successfully applied as cell optical probes⁷ and photothermal reagents,⁸ which show lower cytotoxicity and significantly better biocompatibility than metal-based QDs. However, there are few reports on the

^a School of Chemical Biology and Biotechnology, Peking University Shenzhen Graduate School, Shenzhen, Guangdong, 518055, China.
E-mail: lizg@pkusz.edu.cn

^b SZU-NUS Collaborative Innovation Center for Optoelectronic Science and Technology and Key Laboratory of Optoelectronic Devices and Systems of Ministry of Education and Guangdong Province College of Optoelectronic Engineering, Shenzhen University, Shenzhen 518060, P. R. China. E-mail: hzhang@szu.edu.cn

† Electronic supplementary information (ESI) available. See DOI: 10.1039/c7tb01068k

‡ These authors contributed equally to this work.

biomedical applications of BP-QDs, especially their application as gene delivery systems in the context of cancer treatment.

In the last decade, gene therapy has attracted great attention and is considered as the promising candidate for diseases with extraordinary development, such as cardiovascular diseases, diabetes, immunodeficiency diseases and cancers. However, due to the poor stability and low-efficiency transfection of nucleic acid molecules into cells, gene therapy is still an experimental technique and is currently in the preclinical research stage. Therefore, development of highly efficient and non-toxic gene delivery systems is a major issue for clinical applications.^{14,15}

Herein, we fabricate BP-QDs by liquid phase exfoliation (LPE) and functionalize them with polyelectrolyte polymers (BP-QDs@PAH) to deliver LSD1 siRNA into human ovarian teratocarcinoma PA-1 cells (Scheme 1). PA-1 cells possess pluripotency as stem cells and have been considered as cancer stem cells (CSCs).^{16–18} Lysine-specific demethylase 1 (LSD1, or KDM1A/AOF2), the first discovered histone demethylase,¹⁹ which specifically removes mono- and dimethyl groups from histone H3 lysine 4 (H3K4) and H3 lysine 9 (H3K9) and maintains the pluripotency of embryonic stem cells and cancer stem cells.²⁰ In addition, LSD1 inhibitors can specifically block the growth of ES and EC cells and induce their differentiation but not that of nonpluripotent cells.²¹ Thus, LSD1 has been regarded as a vital potential target for treating cancer *via* targeting CSCs.^{22–24} To our knowledge, our study is the first evidence that BP-QDs can be applied as siRNA delivery systems for gene therapy in CSCs. BP-QDs@PAH core-shell exhibited superior transfection efficiency compared to the commercial delivery reagents (such as Lipofectamine 2000 and Oligofectamine). Furthermore, the results of cell toxicity assessments showed that BP-QDs@PAH had negligible cytotoxicity. Notably, PA-1 cell growth

inhibition rate reached 80% through the synergistic effect of LSD1 siRNA delivered by BP-QDs@PAH and NIR light treatment. As a proof-of-concept study, our findings demonstrated that BP-QDs could be utilized as novel gene delivery systems for efficiently delivering siRNA into cancer cells and showing synergistic photothermal effects.⁸

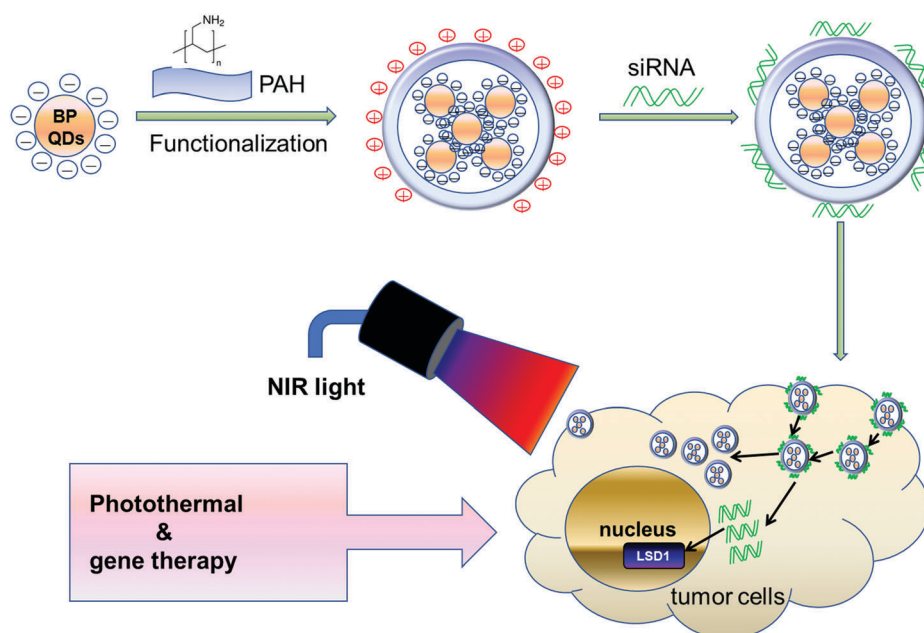
2. Methods and materials

2.1 Preparation of BP-QDs

We employed liquid phase exfoliation (LPE) to obtain BP-QDs.²⁵ The liquid phase exfoliation was considered as a simple but effective technique to synthesize Ultrasmall black phosphorus quantum dots. 20 mg of bulk black phosphorus powder was added to 20 mL of *N*-methyl-2-pyrrolidone (NMP) in a 50 mL sealed conical tube and sonicated with a sonic tip for 3 h at a power of 1200 W. The ultrasonic frequency was from 19 to 25 kHz and the ultrasound probe worked for 2 s with an interval of 4 s. The dispersion was then sonicated in an ultrasonic bath continuously for another 11 h at a power of 300 W. The temperature of the sample solution was kept below 277 K using an ice bath. The resulting dispersion was centrifuged for 20 min at 7000 rpm, and the supernatant containing BPQDs was decanted gently. Then, the BPQD solution was centrifuged for 20 min at 12 000 rpm, and the precipitate was rinsed repeatedly with water and re-suspended in aqueous solution.

2.2 Preparation of BP-QDs@PAH

For siRNA loading, PAH was predissolved in ultrapure DI water (10 mg mL⁻¹). BP-QDs (1 mg mL⁻¹) were mixed with PAH (10 mg mL⁻¹) at a volume ratio of 1 : 1. The mixture was stirred



Scheme 1 Schematic illustration of a combination of photothermal and gene therapies by functional BP-QDs@PAH loaded with siRNA in cancer cells.

for 4 hours at room temperature. Free PAH was removed by centrifugation.

2.3 Gel retardation assay to access the quantity of siRNA delivered by BP-QDs@PAH-based nanocarriers

The siRNA binding ability of the BP-QDs@PAH-based nanocarriers was studied using agarose gel electrophoresis. BP-QDs@PAH (1 mg mL⁻¹) was mixed with siRNA (0.4 mg mL⁻¹) at five different mass ratios (1 μg : 1 μg, 2 μg : 1 μg, 4 μg : 1 μg, 8 μg : 1 μg, 10 μg : 1 μg and 15 μg : 1 μg). Electrophoresis was carried out on a 1% agarose gel with a current of 100 V for 15 min in a TAE buffer solution (40 mM Tris-HCl, 1 v/v% acetic acid, and 1 mM EDTA). The retardation of the complexes was visualized by staining with ethidium bromide and then analyzed on a UV illuminator to show the position of the complex siRNA band relative to that of naked siRNA.

2.4 Tumor cell line and culture

Human ovarian teratocarcinoma cells, PA-1 (CRL-1572, American Type Culture Collection), were maintained in Eagle's Minimum Essential Medium (EMEM, Gibco) supplemented with 10% (v/v) fetal bovine serum (FBS, Hyclone) and penicillin/streptomycin (100 μg mL⁻¹, Gibco). Cells were cultured at 37 °C in a humidified atmosphere with 5% CO₂.

2.5 Flow cytometry

For the flow cytometry of transfection efficiency experiments, PA-1 cells were washed twice with phosphate-buffered saline (PBS) and harvested by trypsinization. Cy3 that served as a luminescent marker (filter set for PE was applied) was used to determine the transfection efficiency quantitatively. The samples were analyzed using a FACScalibur flow cytometer (Becton Dickinson, Mississauga, CA). The transfection efficiency was calculated based on the reported methods^{26,27} by calculating the number of cells in different gates.

2.6 Cell viability test

Cell viability was measured using the MTT (3-(4,5-dimethylthiazol-2-yl)-2,5-diphenyltetrazolium bromide, Sigma) assay. Cells were seeded in a 96-well plate at a density of 5 × 10³ cells per well and incubated with different BP-QD nanocomplexes for indicated time points. For combination with NIR light, PA-1 cells were incubated with BP-QDs@PAH or BP-QDs@PAH-siRNA nanocomplexes for 4 hours, washed with PBS twice, and then irradiated by an 808 nm NIR light at a power density of 1 W cm⁻² for 2 minutes. MTT (5 mg mL⁻¹, 20 μL) in PBS was added and the cells were incubated for 4 hours at 37 °C with 5% CO₂. DMSO (dimethylsulfoxide, 150 μL, Sigma) was then added to solubilize the precipitate with 5 min gentle shaking. Absorbance was measured with a microplate reader (Bio-Rad) at a wavelength of 490 nm. The cell viability was obtained by normalizing the absorbance of the sample well against that from the control well and expressed as a percentage, assigning the viability of non-treated cells as 100%.

2.7 RNA isolation and quantitative RT-PCR

48 hours after transfection, total RNA was extracted from PA-1 cells using TRIzol reagent (Invitrogen) and the amount of RNA was quantitated using a spectrophotometer (Nano-Drop ND-2000). Total RNA (2 μg) was reverse transcribed to cDNA using the reverse transcriptase kit from Takara according to the manufacturer's instructions. The mRNA levels of the target genes were quantified by real time PCR using SYBR green (Takara) in a Bio-Rad CFX Connect real-time PCR system.

2.8 Western blotting

For western blot analysis, cells were seeded in 6-well plates and treated for 24 hours with different BP-QD nanocomplexes as described for the RT-PCR assay. To isolate protein, cells were washed with PBS and harvested using the lysis buffer (50 mM Tris-Cl pH = 6.8, 2% SDS, 6% glycerol, 1% β-mercaptoethanol, 0.004% bromophenol blue). Total cellular protein concentrations were determined using a spectrophotometer (Nano-Drop ND-2000). 20 μg of denatured cellular extracts were resolved using 10% SDS-PAGE gels. Protein bands in the gel were then transferred to nitrocellulose blotting membranes and incubated with appropriate primary antibodies. The antibody dilutions were as follows: 1 : 1000 for LSD1 and 1 : 3000 for histone H3. Membranes were incubated overnight at 4 °C and washed the next day with buffer (1× PBS, 0.05% Tween 20). Goat anti-rabbit secondary antibodies were used for secondary incubation for 1 hour at room temperature. Proteins were then visualized using chemiluminescent substrates.

3. Results and discussion

3.1 Synthesis and preparation of BP-QD based siRNA delivery systems

As a novel compound in 2D nanomaterials in the last two years, black phosphorus (BP) is predicted to be a strong competitor to graphene, due to its uniquely tunable band gap ranging from 0.3 to 2 eV. There are two main ways to produce phosphorene: Scotch-tape-based microcleavage²⁸ and liquid exfoliation.²⁹ BP-QDs used in this research were produced *via* liquid exfoliation (Fig. S1, ESI[†]) with an average diameter of 2.6 nm (Fig. 1A and Fig. S2A, ESI[†]) and a dopant emission peak at 420 nm (Fig. S2B, ESI[†]). The Raman spectra indicated that the structure of QDs was maintained after PAH modification (Fig. 1B). Both BP@PAH and bare BP-QDs showed three prominent Raman peaks. Compared to bare BP-QDs, the BP@PAH was red-shifted by about 3.4, 2.0, and 2.0 cm⁻¹, respectively, which was consistent with previous reports.¹³ BP-QDs@PAH also exhibited an absorption peak at 290 nm as BP-QDs, which was not changed by PAH modification as shown in Fig. S2C (ESI[†]). The zeta potential of the naked BP-QDs was -39.02 ± 0.43 mV (Fig. 1C). After PAH modification, BP-QDs@PAH showed a strong positive charge (33.41 ± 1.05 mV). When siRNAs were loaded onto BP-QDs@PAH with a 15 μg : 1 μg BP-QDs@PAH/siRNA ratio (the optimized ratio, Fig. S2D, ESI[†]), the zeta potential changed to -28.31 ± 1.38 mV. The hydrodynamic diameters of

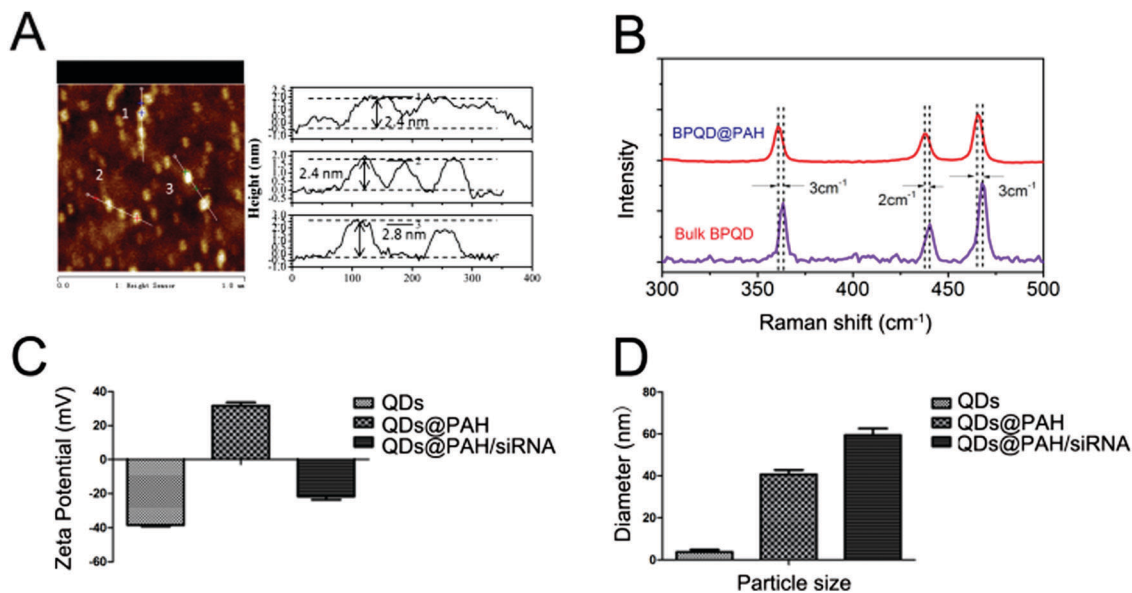


Fig. 1 Characterization of BP-QDs. (A) AFM. (B) Raman spectra of BP-QDs and BP-QDs@PAH. (C) Surface zeta potential and (D) hydrodynamic size of the different BP-QD nanocomplexes. All experiments were performed in duplicates with consistent results. Values are means \pm SEM, $n = 3$. Loading ratio, 15 μg : 1 μg BP-QDs@PAH/siRNA, which was determined by the gel retardation assay shown in Fig. S2D (ESI †). This BP-QDs@PAH/siRNA ratio was used for all subsequent studies. Experimental details are presented in the supplementary experimental section (ESI †).

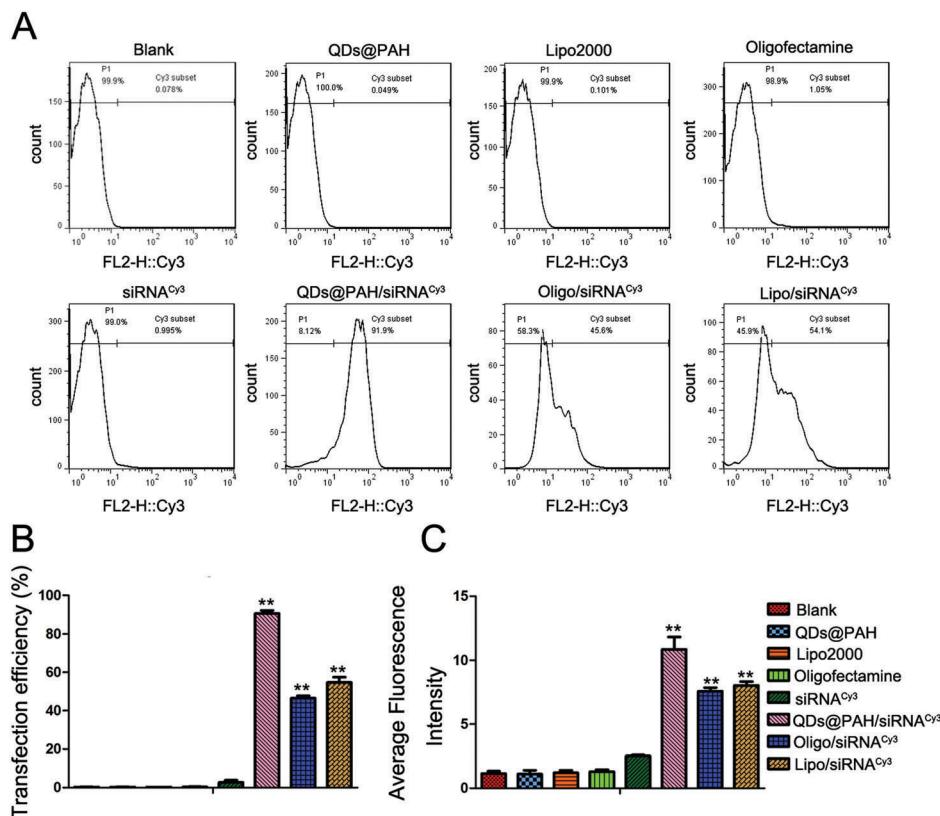


Fig. 2 Flow cytometry evaluations on the transfection efficiencies of PA-1 cells treated with PBS (as blank), QDs@PAH, free LSD1-siRNA^{Cy3}, QDs@PAH/LSD1-siRNA^{Cy3}, Lipofectamine 2000, Lipofectamine 2000/LSD1-siRNA^{Cy3}, Oligofectamine and Oligofectamine/LSD1-siRNA^{Cy3}. (A) Representative dot plot of flow cytometry assays, where the x-axis shows the fluorescence intensities of Cyc3 and the y-axis shows cell counts, respectively. (B and C) Transfection efficiency and average fluorescence intensity from experiments shown in (A). Values are means \pm SEM, $n = 3$, **, $P < 0.01$ vs. control, QDs@PAH and LSD1 siRNA^{Cy3}.

BP-QD nanocomplexes were determined by dynamic light scattering (DLS) (Fig. 1D). Increasing after PAH modification and siRNA loading, the final diameter of BP-QDs@PAH/siRNA was 58 nm, which is within the optimum size range for cellular transfection.^{30,31}

3.2 Cell flow cytometry analysis of BP-QD nanocomplexes

LSD1 participates in gene regulation either as a coactivator by demethylating H3K9me1/2³² or as a corepressor by demethylating H3K4me1/2.³³ Besides, it can also demethylate nonhistone proteins, including p53³⁴ and Dnmt1.³⁵ Importantly, LSD1 can regulate the pluripotency, cell cycle progression, and cellular differentiation of pluripotent embryonic carcinoma/teratocarcinoma cells, such as F9 cells and PA-1 cells.^{18,21} Due to the critical roles of LSD1, in our studies, the specific siRNAs which can target LSD1 gene have been delivered into PA-1 cells by BP-QDs nanodots for gene therapy. As shown in Fig. 2 and Fig. S6 (ESI[†]), the cellular uptake efficiency and intracellular distribution of siRNA^{Cy3} were monitored by flow cytometry analysis (FACS). PA-1 cells were treated with various nanocomplexes for 4 hours before examining by FACS. The cells treated with PBS (as blank), BP-QDs@PAH, free LSD1 siRNA^{Cy3} and two commercial reagents [Lipofectamine 2000 (Lipo2000) and Oligofectamine (Oligo)] were used as positive controls. Fig. 2A and Fig. S6A (ESI[†]) show the representative fluorescence plots

of PA-1 cells treated with different complexes. Fig. 2B, C and Fig. S6B, C (ESI[†]) show the corresponding transfection efficiency and average fluorescence signals in PA-1 cells, respectively. PA-1 cells treated by the BP-QDs@PAH/siRNA^{Cy3} nanocomplex exhibited the strongest Cy3 fluorescence signals, with the highest corresponding transfection efficiency (92.7%). The fluorescence signals were much higher than that of cells treated with the Lipo/siRNA^{Cy3} nanocomplex (48.5%), the oligo/siRNA^{Cy3} nanocomplex (56.9%) or the PAH/siRNA^{Cy3} nanocomplex (44.8%). There were almost no fluorescence signals from negative controls. These results indicated that functionalized BP-QDs could efficiently deliver siRNA into cells.

3.3 Fluorescence microscopy images of BP-QD nanocomplexes in PA-1 cells

To further confirm the delivery efficiency of siRNA by BP-QDs, fluorescence microscopy images were obtained as shown in Fig. 3. The strongest red (Cy3) fluorescence signals were detected from PA-1 cells treated by the BP-QD@PAH/LSD1 siRNA^{Cy3} nanocomplex. As a comparison, weaker fluorescence signals were observed from the cells treated with commercial reagents Lipofectamine 2000–siRNA or Oligofectamine–siRNA nanocomplexes. As expected, no fluorescence signals could be observed from PA-1 cells treated with PBS. These results are consistent with the FACS analysis in Fig. 2A and B and further

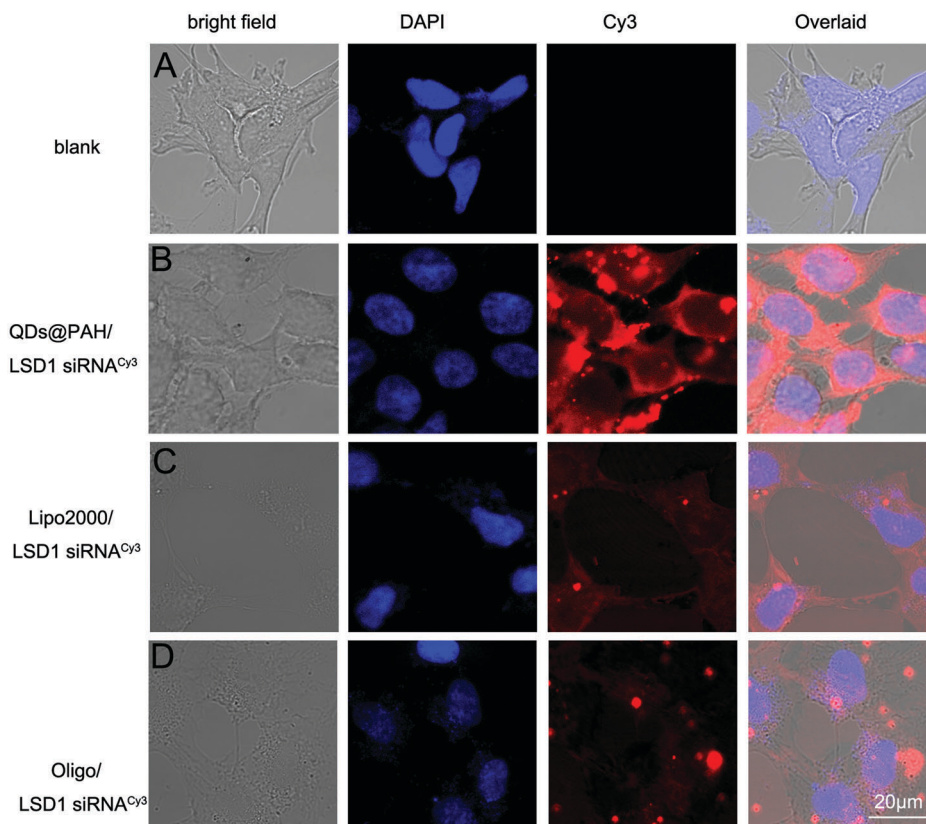


Fig. 3 Fluorescence images of PA-1 cells treated with (A) PBS as the blank control, (B) QDs@PAH/LSD1-siRNA^{Cy3}, (C) Lipo2000/LSD1-siRNA^{Cy3} and (D) Oligo/LSD1-siRNA^{Cy3} after four hours of treatment. The cell nucleus is stained with DAPI (pseudo-colored in blue) and signals from Cy3 are assigned in red, respectively.

confirm the superior delivery efficiency of BP-QD based nanocarriers compared to the commercial reagents.

3.4 Gene expression evaluations of PA-1 cells treated with different BP-QDs nanocomplexes

Following the flow cytometry analysis and fluorescence microscopy, the results in Fig. 4 and Fig. S5 (ESI[†]) have shown the degree of gene knockdown of LSD1 at the mRNA level and protein level in PA-1 cells treated by different BP-QD nanocomplexes. Compared with PBS or BP-QDs@PAH, cells treated with BP-QDs@PAH/siRNA showed a remarkable inhibition rate of LSD1 gene expression. On the other hand, cells treated with BP-QDs@PAH or BP-QDs@PAH/scramble siRNA showed no obvious changes of LSD1 at both mRNA and protein levels. Moreover, the mRNA level of SOX2 has been down-regulated obviously in cells treated with BP-QDs@PAH/siRNA, which was the key substrate of LSD1^{18,21,36} and further demonstrated the ablation of LSD1 by BP-QDs@PAH/siRNA. According to the RT-PCR analysis and western blotting analysis, BP-QD-based nanocarriers showed great potential as effective siRNA delivery

systems to deliver siRNA in cells and induce target gene knockdown for gene therapy in cancer and other diseases.

3.5 Viability of PA-1 cells treated with different BP-QD nanocomplexes

LSD1 plays essential roles in maintaining the pluripotency and proliferation of stem cells and cancer stem cells.^{20,37,38} Based on the gene knockdown results in Fig. 4, the BP-QDs@PAH/LSD1 siRNA nanocomplex can sufficiently suppress the expression of the LSD1 gene. Subsequently, we further examined the cell growth treated by different BP-QD nanocomplexes (Fig. 5 and Fig. S7, ESI[†]). To assess the toxicity of naked BP-QDs@PAH/QDs, PA-1 cells were treated with different concentrations of BP-QDs@PAH/QDs ranging from 0.1 mg mL⁻¹ to 5 mg mL⁻¹ for 48 hours. The cell viability was maintained around 80% even at the highest concentration (5 mg mL⁻¹), which demonstrated the good biocompatibility and low toxicity of BP-QDs@PAH. However, PAH was more cytotoxic than BP-QDs@PAH with a half maximal inhibitory concentration (IC₅₀) of around 4 μg mL⁻¹ (Fig. S7, ESI[†]). As shown in Fig. 5, compared to PBS-treated cells (as the blank control), there was negligible inhibition of the cell growth in these cells treated with BP-QDs@PAH/scramble siRNA for 48 hours. In contrast, obvious inhibition was found in cells treated with BP-QDs@PAH/LSD1 siRNA (62.1%). It was worth noting that the strongest inhibition rate (over 80%) was observed for the combination of BP-QDs@PAH/LSD1 siRNA nanocomplexes and 808 nm NIR light, due to the excellent NIR photothermal performance of BP-QDs (Fig. 5C and Fig. S3, ESI[†]). These results suggested that BP-QDs play synergistic roles in both photothermal and gene therapy.

Cancers figure among the leading causes of morbidity and mortality worldwide, impacting 14 million people each year depending on the WHO reports. The poor prognosis of many types of tumors including breast, colon, and ovary tumors is not only related to the high proliferative activity of tumor cells³⁹ but also to metastasis and drug-resistance.⁴⁰ One emerging model for the development of drug-resistance and metastasis of tumors related to a self-renewing malignant primogonitor known as cancer stem cells (CSCs). CSCs can generate an abnormal organ of the tissue from which they derive, with a series of cell types at distinct stages of differentiation.⁴¹ Thus, due to the failure of deracinating CSCs, the cancers figure relapse after remission. The PA-1 cell line, derived from human ovarian teratocarcinoma cells, is a well-accepted model for studying cancer cell stemness and expresses endogenous, non-functional wild-type p53.^{42–44} However, due to the low transfection efficiency of the normal commercial delivery agents in PA-1 cells or stem cells, new delivery systems with low toxicity and high transfection efficiency are urgently needed. In our study, we prepared the multifunctional BP quantum dots (BP-QDs)-based siRNA nanocarriers, which exhibited good transfection efficiency. Furthermore, BP-QDs possess good biocompatibility and low cytotoxicity at concentrations as high as 5 mg mL⁻¹. Therefore, BP-QD nanoparticles could be potentially translated for clinical research application in cancer therapy.

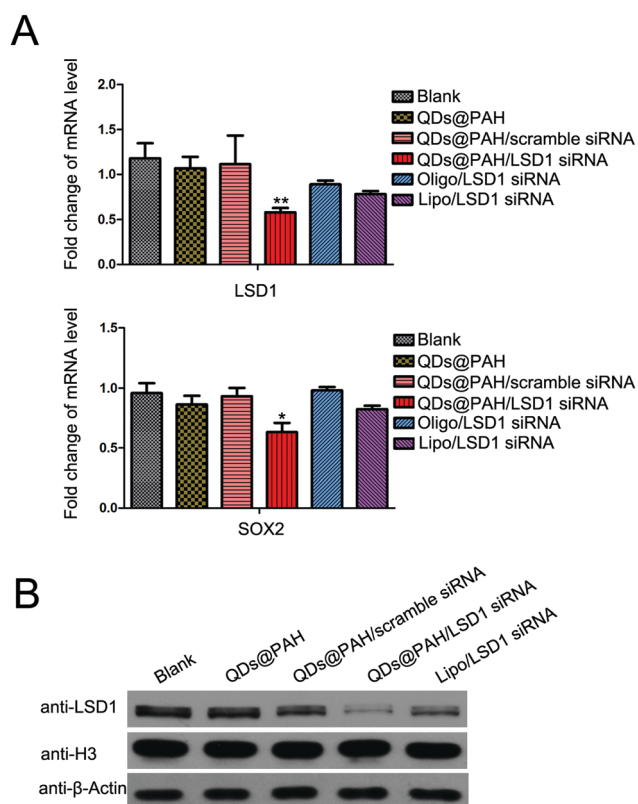


Fig. 4 Gene expression evaluations of PA-1 cells treated with different BP-QD nanocomplexes. PA-1 cells (cultured in 6-well plate) were treated with PBS, QDs@PAH (20 μg), QDs@PAH/LSD1-siRNA (20 μg/1.3 μg), QDs@PAH/scramble-siRNA, Lipo2000/LSD1-siRNA and Oligo/LSD1-siRNA for 4 hours, and then all the cells were washed with PBS and re-incubated in fresh cell medium for an additional 44 hours. (A) Relative mRNA expression levels detected by RT-PCR. (B) Relative protein expression levels detected by western blotting. H3 and β-actin were used as the protein loading control for samples. Values are means ± SEM, *n* = 3; ***P* < 0.01 vs. control and QDs@PAH.

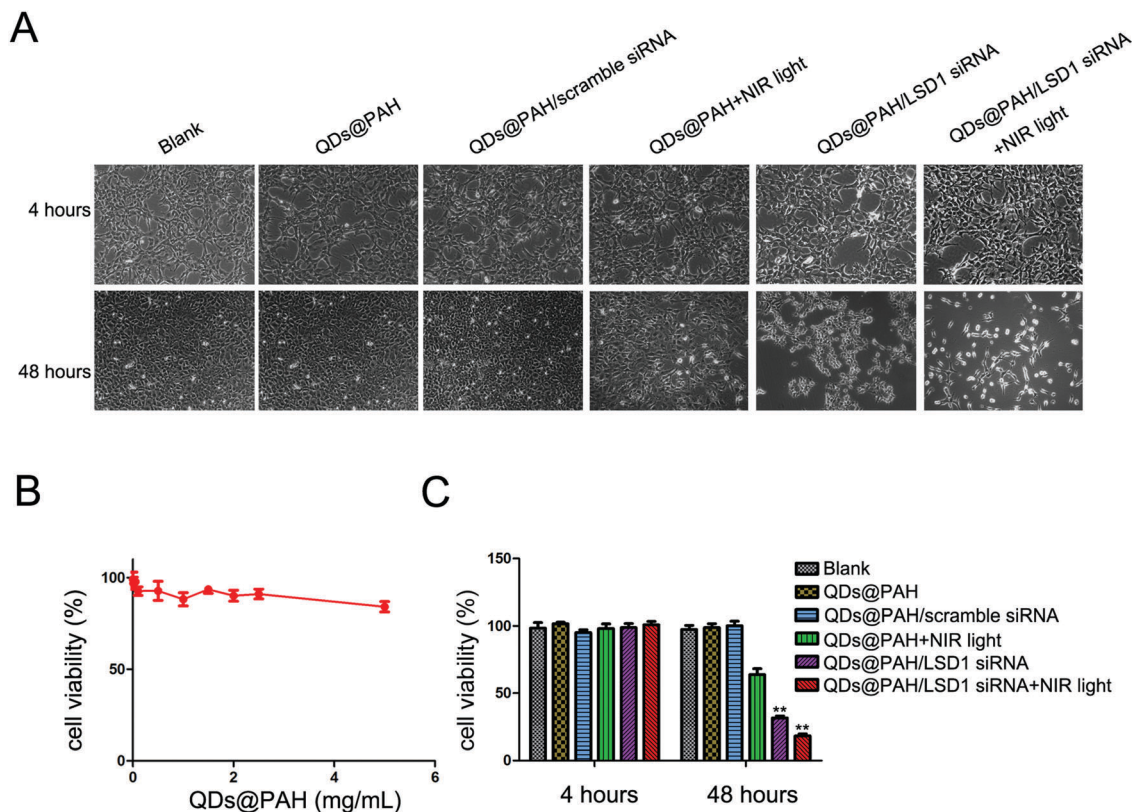


Fig. 5 Cell viability tests of different BP-QD nanocomplexes with NIR light. The growth of PA-1 cells (cultured in 6-well plate) was inhibited profoundly by the BP-QDs@PAH/siRNA nanocomplex with NIR light. PA-1 cells were treated with PBS, QDs@PAH, QDs@PAH/LSD1-siRNA, and QDs@PAH/scramble-siRNA for 4 hours. NIR light (808 nm continuous-wave NIR laser with a power density of 1 W cm^{-2} and a spot size of 5 mm) was utilized to treat QDs@PAH and QDs@PAH/LSD1-siRNA for 5 minutes. Then all the cells were washed with PBS and re-incubated in fresh cell medium for designated times. Phase contrast microscopy images (A) and relative cell viabilities (C) of PA-1 cells treated with different BP-QD nanocomplexes without or with NIR light for 4 and 48 hours. (B) Viability of cells after incubation with BP-QDs@PAH at varying concentrations up to 5 mg mL^{-1} for 48 hours. Values are means \pm SEM, $n = 3$; $^{**}P < 0.01$ vs. control and QDs@PAH.

4. Conclusion

In summary, for the first time, we developed a novel nanodrug based on BP-QDs for CSCs with a combination of photothermal therapy and gene therapy. Here, the delivery of LSD1 siRNA by BP-QDs@PAH shows a high rate of internalization in PA-1 cells and exhibits a 80% inhibition rate of cell proliferation under NIR light. On the other hand, negligible toxicity was observed in cells treated with BP-QDs. In conclusion, a BP-QD-based siRNA delivery system exhibits superior transfection efficiency, biocompatibility and non-toxicity, which shows great potential to be used in biomedical research for cancer therapy (especially the CSC therapy) and other disease treatments. A further *in vivo* study of BP-QD-siRNA is undergoing in our lab and will be reported in due course.

Competing interests

The authors have declared that no competing interest exists.

Acknowledgements

This work was supported by the National Natural Science Foundation of China (Grants 21372023 and 81572198),

MOST (2015DFA31590), the Shenzhen Science and Technology Innovation Committee (JSGG20140519105550503, JCYJ20150-331100849958, JCYJ20150403101146313, JCYJ20160301111338144, JCYJ20160331115853521, and JSGG20160301095829250), and the Shenzhen Peacock Program (KQTD201103). Dr Feng Yin was supported in part by the Postdoctoral Fellowship of Peking-Tsinghua Center for Life Sciences.

References

- 1 L. K. Li, Y. J. Yu, G. J. Ye, Q. Q. Ge, X. D. Ou, H. Wu, D. L. Feng, X. H. Chen and Y. B. Zhang, *Nat. Nanotechnol.*, 2014, **9**, 372–377.
- 2 Y. Chen, G. B. Jiang, S. Q. Chen, Z. N. Guo, X. F. Yu, C. J. Zhao, H. Zhang, Q. L. Bao, S. C. Wen, D. Y. Tang and D. Y. Fan, *Opt. Express*, 2015, **23**, 12823–12833.
- 3 H. R. Mu, S. H. Lin, Z. C. Wang, S. Xiao, P. F. Li, Y. Chen, H. Zhang, H. F. Bao, S. P. Lau, C. X. Pan, D. Y. Fan and Q. L. Bao, *Adv. Opt. Mater.*, 2015, **3**, 1447–1453.
- 4 F. N. Xia, H. Wang and Y. C. Jia, *Nat. Commun.*, 2014, **5**, 4458.
- 5 D. Hanlon, C. Backes, E. Doherty, C. S. Cucinotta, N. C. Berner, C. Boland, K. Lee, A. Harvey, P. Lynch,

- Z. Gholamvand, S. F. Zhang, K. P. Wang, G. Moynihan, A. Pokle, Q. M. Ramasse, N. McEvoy, W. J. Blau, J. Wang, G. Abellan, F. Hauke, A. Hirsch, S. Sanvito, D. D. O'Regan, G. S. Duesberg, V. Nicolosi and J. N. Coleman, *Nat. Commun.*, 2015, **6**, 8563.
- 6 V. Tran, R. Soklaski, Y. F. Liang and L. Yang, *Phys. Rev. B: Condens. Matter Mater. Phys.*, 2014, **89**, 235319.
- 7 H. U. Lee, S. Y. Park, S. C. Lee, S. Choi, S. Seo, H. Kim, J. Won, K. Choi, K. S. Kang, H. G. Park, H. S. Kim, H. R. An, K. H. Jeong, Y. C. Lee and J. Lee, *Small*, 2016, **12**, 214–219.
- 8 Z. B. Sun, H. H. Xie, S. Y. Tang, X. F. Yu, Z. N. Guo, J. D. Shao, H. Zhang, H. Huang, H. Y. Wang and P. K. Chu, *Angew. Chem., Int. Ed.*, 2015, **54**, 11526–11530.
- 9 C. Sun, L. Wen, J. Zeng, Y. Wang, Q. Sun, L. Deng, C. Zhao and Z. Li, *Biomaterials*, 2016, **91**, 81–89.
- 10 W. Chen, J. Ouyang, H. Liu, M. Chen, K. Zeng, J. Sheng, Z. Liu, Y. Han, L. Wang, J. Li, L. Deng, Y. N. Liu and S. Guo, *Adv. Mater.*, 2017, **29**, 1603864.
- 11 W. Tao, X. Zhu, X. Yu, X. Zeng, Q. Xiao, X. Zhang, X. Ji, X. Wang, J. Shi, H. Zhang and L. Mei, *Adv. Mater.*, 2017, **29**, 1603276.
- 12 X. H. Niu, Y. H. Li, H. B. Shu and J. L. Wang, *J. Phys. Chem. Lett.*, 2016, **7**, 370–375.
- 13 C. Yu, X. Li, F. Zeng, F. Zheng and S. Wu, *Chem. Commun.*, 2013, **49**, 403–405.
- 14 H. Wang, W. Chen, H. Xie, X. Wei, S. Yin, L. Zhou, X. Xu and S. Zheng, *Chem. Commun.*, 2014, **50**, 7806–7809.
- 15 Z. Yu, B. Yu, J. B. Kaye, C. Tang, S. Chen, C. Dong and B. Shen, *Nano LIFE*, 2014, **4**, 1441016.
- 16 S. Peng, N. J. Maihle and Y. Huang, *Oncogene*, 2010, **29**, 2153–2159.
- 17 K. Moitra, H. Lou and M. Dean, *Clin. Pharmacol. Ther.*, 2011, **89**, 491–502.
- 18 F. Yin, R. F. Lan, X. M. Zhang, L. Y. Zhu, F. F. Chen, Z. S. Xu, Y. Q. Liu, T. Ye, H. Sun, F. Lu and H. Zhang, *Mol. Cell. Biol.*, 2014, **34**, 158–179.
- 19 Y. Shi, F. Lan, C. Matson, P. Mulligan, J. R. Whetstone, P. A. Cole and R. A. Casero, *Cell*, 2004, **119**, 941–953.
- 20 M. A. Glozak and E. Seto, *Oncogene*, 2007, **26**, 5420–5432.
- 21 J. Wang, F. Lu, Q. Ren, H. Sun, Z. S. Xu, R. F. Lan, Y. Q. Liu, D. Ward, J. M. Quan, T. Ye and H. Zhang, *Cancer Res.*, 2011, **71**, 7238–7249.
- 22 H. J. Xie, J. H. Noh, J. K. Kim, K. H. Jung, J. W. Eun, H. J. Bae, M. G. Kim, Y. G. Chang, J. Y. Lee, H. Park and S. W. Nam, *PLoS One*, 2012, **7**, e34265.
- 23 J. S. Wu, L. Gherghel, M. D. Watson, J. X. Li, Z. H. Wang, C. D. Simpson, U. Kolb and K. Mullen, *Macromolecules*, 2003, **36**, 7082–7089.
- 24 F. L. Delarue, J. Adnane, B. Joshi, M. A. Blaskovich, D. A. Wang, J. Hawker, F. Bizouarn, J. Ohkanda, K. Zhu, A. D. Hamilton, S. Chellappan and S. M. Sebti, *Oncogene*, 2007, **26**, 633–640.
- 25 X. Zhang, H. M. Xie, Z. D. Liu, C. L. Tan, Z. M. Luo, H. Li, J. D. Lin, L. Q. Sun, W. Chen, Z. C. Xu, L. H. Xie, W. Huang and H. Zhang, *Angew. Chem., Int. Ed.*, 2015, **54**, 3653–3657.
- 26 G. M. Lin, R. Hu, W. C. Law, C. K. Chen, Y. C. Wang, H. L. Chin, Q. T. Nguyen, C. K. Lai, H. S. Yoon, X. M. Wang, G. X. Xu, L. Ye, C. Cheng and K. T. Yong, *Small*, 2013, **9**, 2757–2763.
- 27 F. Yin, C. B. Yang, Q. Q. Wang, S. W. Zeng, R. Hu, G. M. Lin, J. L. Tian, S. Y. Hu, R. F. Lan, H. S. Yoon, F. Lu, K. Wang and K. T. Yong, *Theranostics*, 2015, **5**, 818–833.
- 28 H. Liu, A. T. Neal, Z. Zhu, Z. Luo, X. F. Xu, D. Tomanek and P. D. Ye, *ACS Nano*, 2014, **8**, 4033–4041.
- 29 A. H. Woomer, T. W. Farnsworth, J. Hu, R. A. Wells, C. L. Donley and S. C. Warren, *ACS Nano*, 2015, **9**, 8869–8884.
- 30 R. Sinha, G. J. Kim, S. Nie and D. M. Shin, *Mol. Cancer Ther.*, 2006, **5**, 1909–1917.
- 31 H. K. Sajja, M. P. East, H. Mao, Y. A. Wang, S. Nie and L. Yang, *Curr. Drug Discovery Technol.*, 2009, **6**, 43–51.
- 32 E. Metzger, M. Wissmann, N. Yin, J. M. Muller, R. Schneider, A. H. F. M. Peters, T. Gunther, R. Buettner and R. Schule, *Nature*, 2005, **437**, 436–439.
- 33 M. G. Lee, C. Wynder, N. Cooch and R. Shiekhhattar, *Nature*, 2005, **437**, 432–435.
- 34 J. Huang, R. Sengupta, A. B. Espejo, M. G. Lee, J. A. Dorsey, M. Richter, S. Opravil, R. Shiekhhattar, M. T. Bedford, T. Jenuwein and S. L. Berger, *Nature*, 2007, **449**, U105–U180.
- 35 J. Wang, S. Hevi, J. K. Kurash, H. Lei, F. Gay, J. Bajko, H. Su, W. T. Sun, H. Chang, G. L. Xu, F. Gaudet, E. Li and T. Chen, *Nat. Genet.*, 2009, **41**, 125–129.
- 36 X. M. Zhang, F. Lu, J. Wang, F. Yin, Z. S. Xu, D. D. Qi, X. H. Wu, Y. W. Cao, W. H. Liang, Y. Q. Liu, H. Sun, T. Ye and H. Zhang, *Cell. Rep.*, 2013, **5**, 445–457.
- 37 Y. Wang, H. Zhang, Y. P. Chen, Y. M. Sun, F. Yang, W. H. Yu, J. Liang, L. Y. Sun, X. H. Yang, L. Shi, R. F. Li, Y. Y. Li, Y. Zhang, Q. Li, X. Yi and Y. F. Shang, *Cell*, 2009, **138**, 660–672.
- 38 T. F. Lv, D. M. Yuan, X. H. Miao, Y. L. Lv, P. Zhan, X. K. Shen and Y. Song, *PLoS One*, 2012, **7**, e35065.
- 39 I. Khalifeh, A. R. Munkarah, V. Schimpf, R. Morris, W. D. Lawrence and R. Ali-Fehmi, *Int. J. Gynecol. Pathol.*, 2005, **24**, 228–234.
- 40 A. P. Singh, S. Senapati, M. P. Ponnusamy, M. Jain, S. M. Lele, J. S. Davis, S. Remmenga and S. K. Batra, *Lancet Oncol.*, 2008, **9**, 1076–1085.
- 41 P. Dalerba, R. W. Cho and M. F. Clarke, *Annu. Rev. Med.*, 2007, **58**, 267–284.
- 42 Y. Yaginuma and H. Westphal, *Cancer Res.*, 1992, **52**, 4196–4199.
- 43 N. C. Reich, M. Oren and A. J. Levine, *Mol. Cell. Biol.*, 1983, **3**, 2143–2150.
- 44 L. Wang, Q. Wu, P. Qiu, A. Mirza, M. McGuirk, P. Kirschmeier, J. R. Greene, Y. Wang, C. B. Pickett and S. Liu, *J. Biol. Chem.*, 2001, **276**, 43604–43610.